

Tuning the morphology of self-assembled nanostructures of amphiphilic tetra(*p*-hydroxyphenyl)porphyrins with hydrogen bonding and metal–ligand coordination bonding†

Guifen Lu, Xiaomei Zhang,* Xue Cai and Jianzhuang Jiang*

Received 11th November 2008, Accepted 26th January 2009

First published as an Advance Article on the web 27th February 2009

DOI: 10.1039/b820127g

Typical amphiphilic metal-free tetrakis(4-hydroxyphenyl)porphyrin H₂THPP (**1**) and tetrakis(4-hydroxyphenyl)porphyrinato copper complex CuTHPP (**2**) were fabricated into organic nanostructures by a phase-transfer method. Their self-assembly properties in aqueous solution have been comparatively studied with those of tetra(phenyl)porphyrin H₂TPP (**3**) by electronic absorption and Fourier transform infrared (FT-IR) spectroscopy, transmission electronic microscopy (TEM), scanning electronic microscopy (SEM), and X-ray diffraction (XRD) techniques. Experimental results reveal different molecular packing models in these aggregates, which in turn result in self-assembled nanostructures with different morphologies from nano-scale hollow spheres for **1**, nanoribbons for **2**, to nanobelts for **3**. The present study, representing part of our continuous efforts towards understanding the relationship between synergistic interplay among noncovalent interactions such as the π – π interaction, metal–ligand coordination bonding, and hydrogen bonding in controlling and tuning the morphology of self-assembled nanostructures of tetrapyrrole derivatives, will provide information helpful for preparing self-assembled nanostructures with controlled molecular packing conformations and morphologies through molecular modification.

Introduction

Self-assembly of functional organic molecules into well-defined organized structures has attracted considerable research interest due to their versatile applications in nanoscience and nanotechnology in recent years.^{1,2} Self-assembly is a natural and spontaneous process occurring mainly through noncovalent interactions such as π – π interaction, van der Waals, hydrogen bonding, hydrophilic/hydrophobic, electrostatic, and metal–ligand coordination bonding. On the basis of different noncovalent interactions, a wide variety of nanostructures such as wires,³ belts,⁴ vesicles,⁵ and tubes⁶ have been fabricated from various functional molecules. Among which, conjugated molecular systems have been recognized as attractive building blocks for supramolecular self-assemblies towards construction of functional nanodevices.

Taking the natural system as a blueprint, tetrapyrrole derivatives including both porphyrins and their non-naturally occurring analogues phthalocyanines as the representatives of functional molecular materials with large conjugated electronic molecular structures have attracted great research interest in the field of organic nanostructures. Over the last decade, great efforts have been devoted to fabricating tetrapyrroles into various kinds of nanostructures with different morphologies due to their various potential applications. For example, hollow capsules produced from amphiphilic porphyrin compounds showed the potential for promising applications in drug delivery agents and guest-entrapping material.^{7,8} Cooperation between cationic/anionic porphyrins and optically active DNA with opposite charge induces the formation of a chiral heteroassembly, which appears to have “life” that is independent from the DNA template but retains “memory” of the shape of the “mold” used during its formation.⁹ Meanwhile metalloporphyrin assemblies have been investigated as models of the light-harvesting antenna complexes and porous materials.^{10–13} For example, an artificial ring composed of Zn(II)-porphyrin with *ca.* 40 nm diameter, which is in close analogy to that of the natural light-harvesting complexes, was reported by Kobuke and Takahashi.¹⁴ A novel metalloporphyrin network of [CoT(*p*-CO₂)PPCo_{1.5}] (designated as PIZA-1 for porphyrinic Illinois zeolite analogue no.1) was revealed to exhibit highly selective and reversible absorption properties towards various organic molecules.¹⁵ The aggregation behavior of phthalocyanines, especially crown ether substituted phthalocyanines, has been extensively studied.^{16–21} For example, the phthalocyanine possessing four crown ether moieties and eight chiral alkoxy side chains has been readily self-assembled into long fibres.¹⁷ Nevertheless, very recently this group has

Department of Chemistry, Shandong University, Jinan, 250100, P. R. China. E-mail: jzjiang@sdu.edu.cn; Fax: +86 531 8856 4464; Tel: +86 531 8856 4088

† Electronic supplementary information (ESI) available: Electronic absorption data for the porphyrin derivatives **1–3** in homogeneous solution and their self-assemblies (Table S1); IR spectra of compound **1**, and aggregates of compound **1** with nano-scale hollow sphere morphology formed in water in the region 400–1800 cm^{−1} with 2 cm^{−1} resolution; IR spectra of compounds **2**, and aggregates of compound **2** with nanoribbon morphology formed in water in the region 400–1800 cm^{−1} with 2 cm^{−1} resolution; IR spectra of compound **3**, and aggregates of compound **3** with nanobelt morphology formed in methanol in the region 400–1800 cm^{−1} with 2 cm^{−1} resolution; preparation of tetrakis(4-hydroxyphenyl)porphyrinato copper complex CuTHPP (**2**); X-ray photoelectron spectra of compound **2** and its aggregates deposited on silicon surface. See DOI: 10.1039/b820127g

incorporated different numbers of acetylsulfanylpenyloxy and hydroxyl groups, respectively, onto the meso-substituted phenyl groups of the porphyrin ligand in 5,15-di[4-(5-acetylsulfanylpenyloxy)phenyl]porphyrinato zinc and mixed (phthalocyaninato)(porphyrinato) europium triple-decker complexes to tune the inter-molecular interactions.^{22,23} Cooperation and/or competition between the intermolecular π - π interaction and hydrogen bonding/metal-ligand coordination bonding for 5,15-di[4-(5-acetylsulfanylpenyloxy)phenyl]porphyrinato zinc and sandwich mixed (phthalocyaninato)(porphyrinato) europium triple-decker compounds result in the formation of nanostructures with different morphologies. It is worth pointing out that despite the availability of a rich toolbox of noncovalent interactions, it still remains a puzzle for chemists and material scientists to understand the effect of the synergistic interplay of different noncovalent interactions on controlling and tuning the morphology of organic self-assembled nanostructures.

Due to the great potential applications in photosensitizers and photodynamic therapy, typical amphiphilic porphyrin derivatives have attracted research attention. For example, meso-tetrakis(4-hydroxyphenyl)porphyrin was incorporated into sub-150 nm biodegradable nanoparticles using the emulsification diffusion technique in order to perform sterilization.^{24,25} Associated with the square-planar molecular symmetry, the capacity to coordinate with various metal centers, and the self-complementarity of π - π interaction in cooperation with hydrogen bonding due to the terminal hydroxyl functional groups, the tetrakis(4-hydroxyphenyl)porphyrin derivatives are expected to provide a unique and versatile platform for the construction of supramolecular structures. When metal ions preferring a coordination number of 5 or 6 are introduced into the central hole of the metal-free porphyrin ligand, the newly formed complexes should provide novel systems for preparing supramolecular structures on the basis of metal-ligand coordination bonding in addition to the π - π interaction and hydrogen bonding due to the axial coordination between the hydroxyl group and the central metal ion. In the present paper, we describe the self-assembly properties of typical amphiphilic metal-free tetrakis(4-hydroxyphenyl)porphyrin H₂THPP (**1**) and tetrakis(4-

hydroxyphenyl)porphyrinato copper complex CuTHPP (**2**), Fig. 1. Comparative studies with the behavior of metal-free tetraphenylporphyrin H₂TPP (**3**) reveal that introduction of four hydroxyl groups onto the meso-attached phenyl groups of the porphyrin ligand and in particular the hexa-coordinated copper ion into the porphyrin central hole leads to the formation of nanostructures with different morphologies, indicating the effect of a synergistic interplay among noncovalent interactions such as π - π interaction, hydrogen bonding, and metal-ligand coordination bonding in controlling and tuning the morphology of self-assembled nanostructures of porphyrin compounds. The present study represents part of our continuous efforts towards understanding the synergistic interplay between noncovalent interactions on controlling and tuning the morphology of self-assembled nanostructures of tetrapyrrole derivatives and also provides information helpful on preparing self-assembled nanostructures with controlled molecular packing conformation and morphology through molecular modification.

Results and discussion

Molecular design, synthesis, and characterization

In addition to the weak van der Waals force, the dominant intermolecular interaction among metal free tetra(phenyl)porphyrins H₂TPP (**3**) with a large conjugated molecular structure is π - π interaction. Incorporation of hydroxyl groups onto the meso-attached phenyl groups of the porphyrin ligand therefore induces additional hydrogen bonding interactions among the molecules of metal-free tetrakis(4-hydroxyphenyl)porphyrin H₂THPP (**1**), which will in turn result in novel supramolecular structures due to the cooperation and/or competition between the intermolecular π - π interaction and hydrogen bonding. When the copper ion, which prefers a coordination number of 6, is introduced into the central hole of the tetrakis(4-hydroxyphenyl)porphyrin ligand, further additional intermolecular metal-ligand coordination bonding interaction is induced for the newly formed complex CuTHPP (**2**) due to the axial coordination between the hydroxyl group and the metal center.

Metal-free tetrakis(4-hydroxyphenyl)porphyrin H₂THPP (**1**) was prepared according to the published procedure.^{26,27} The copper complex CuTHPP (**2**) was obtained in good yield from the reaction between metal-free porphyrin H₂THPP (**1**) and Cu(AcO)₂·H₂O in refluxing DMF.²⁸ For the purpose of comparative studies, metal-free tetra(phenyl)porphyrin derivative H₂TPP (**3**) was similarly synthesized. A satisfactory elemental analysis result was obtained for the newly prepared copper complex CuTHPP (**2**) after repeatedly column chromatographic purification and recrystallization. The MALDI-TOF mass spectrum of this compound clearly showed an intense signal for the protonated molecular ion (M + H)⁺. This compound was also characterized by electronic absorption and IR spectroscopy.

Electronic absorption spectra

Extensive studies have revealed that discrimination between the *H* versus *J* porphyrin-porphyrin stacking modes can be easily achieved by electronic absorption spectroscopic examination.²⁹ Fig. 2A and B display the electronic absorption spectra of

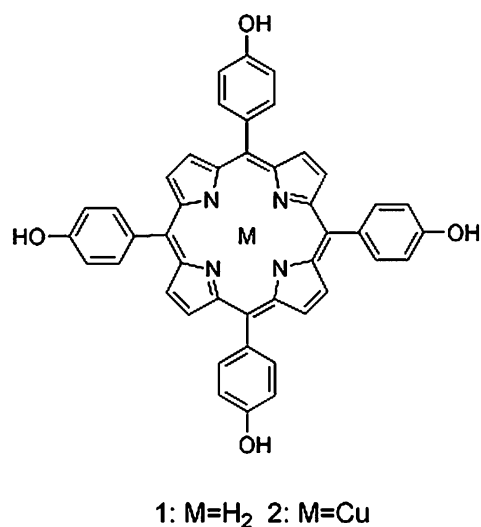


Fig. 1 Schematic molecular structure of amphiphilic porphyrins **1** and **2**.

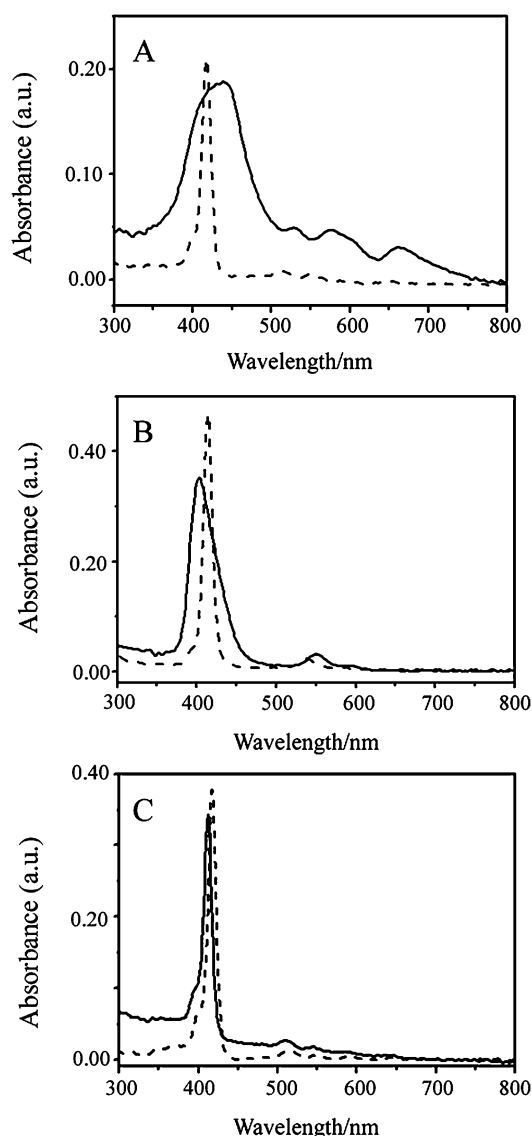


Fig. 2 Electronic absorption spectra of (A) **1** in CH_3OH ($5 \times 10^{-7} \text{ mol L}^{-1}$, dashed line) and its self-assembled nano-scale hollow spheres formed in water ($1 \times 10^{-6} \text{ mol L}^{-1}$, solid line); (B) **2** in CH_3OH ($1 \times 10^{-6} \text{ mol L}^{-1}$, dashed line) and its self-assembled nanoribbons formed in water ($5 \times 10^{-6} \text{ mol L}^{-1}$, solid line); (C) **3** in CHCl_3 ($5 \times 10^{-7} \text{ mol L}^{-1}$, dashed line) and its self-assembled nanobelts formed in CH_3OH ($1 \times 10^{-6} \text{ mol L}^{-1}$, solid line).

compounds **1** and **2** dissolved in methanol and their self-assembled nanostructures formed in water, respectively. For the purpose of comparative studies, the electronic absorption spectra of metal free analogue H_2THPP (**3**) in CHCl_3 and dispersed in methanol are also shown in Fig. 2C. In line with H_2THPP (**3**) in CHCl_3 ,³⁰ the metal-free porphyrin H_2THPP (**1**) shows a typical non-aggregate molecular electronic absorption spectrum with the Soret band at 418 nm and Q absorption bands at 516, 554, 593, and 648 nm, respectively, in methanol.²⁷ When dispersed in water and methanol, respectively, molecules of both metal-free porphyrins **1** and **3** undergo aggregation, resulting in distinct change in their electronic absorption spectra, Fig. 2A and C. In comparison with those in CHCl_3 , both the Soret and Q absorption bands for the aggregates of **3** in methanol are blue-

shifted, Table S1 (ESI[†]), because of the π - π interaction between the metal-free porphyrin molecules of H_2THPP (**3**). In contrast, incorporation of hydroxyl groups onto the meso-attached phenyl groups of the porphyrin ligand induces different changes in the electronic absorption spectrum of amphiphilic metal-free porphyrin H_2THPP (**1**) under aggregation. When dispersed in water, all the absorption peaks for **1** are significantly broadened with the Soret and Q absorption bands red-shifting to 438, 529, 576, 605, and 661 nm from 418, 514, 550, 595, and 647 nm in methanol. These results imply intensified molecular interaction between porphyrin molecules in the nanostructure of **1** due to the cooperation of hydrogen bonding between adjacent porphyrin molecules together with the intermolecular π - π stacking. This was indeed verified by the IR spectroscopic and XRD results as detailed below.

Upon complexation with the six-coordinate copper ion, the increase in the molecular symmetry induces change in the electronic absorption spectrum from typical features for metal-free tetrakis(4-hydroxyphenyl)porphyrin **1** to those for typical porphyrinato metal species **2**. Fig. 2B shows the electronic absorption spectrum of typical non-aggregated metal porphyrin species CuTHPP (**2**) in methanol with a strong sharp Soret band at 414 nm and two weak Q absorptions at 540 and 576 nm, respectively. However, when dispersed in water, the peaks are significantly broadened and a blue shift of the Soret band by 11 nm (with the porphyrin Q bands remained unchanged or slightly blue-shifted, respectively) indicates the effect of the central copper ion on the molecular packing conformation in aggregates due to the introduction of additional metal-ligand (Cu-O) coordination between neighboring molecules.

On the basis of Kasha's exciton theory,³¹ blue shifts in the main absorption bands of the metal-free tetra(phenyl)porphyrin **3** upon aggregation are typically a sign of the effective π - π interaction between metal-free porphyrin molecules, indicating the formation of *H* aggregates from the compound in methanol. This is in line with the result revealed by single crystal diffraction analysis of the structure of this compound.³² In contrast, the red-shift in the main absorption bands of compound **1** upon aggregation in water reveals the *J*-aggregate nature in the nano-scale hollow spheres formed from **1**. Nevertheless, the blue-shifted absorption band in the main electronic absorption spectrum of porphyrinato copper complex CuTHPP (**2**) upon aggregation in water implies the molecules of this compound are enforced to adopt the *H* aggregation mode due to the additional Cu-O metal-ligand coordination bonding interaction between the hydroxyl group of one molecule and the copper center of a neighboring porphyrinato copper molecule. These results indicate the dominant role of π - π interaction between the molecules of metal-free tetra(phenyl)porphyrin **3** but of hydrogen bonding for metal-free tetrakis(4-hydroxyphenyl)porphyrin **1** and metal-ligand coordination bonding interaction for tetrakis(4-hydroxyphenyl)porphyrinato copper complex **2**, with the cooperation of intermolecular π - π interaction for **1** and intermolecular π - π interaction as well as hydrogen bonding for **2**, revealing the effect of a synergistic interplay among noncovalent interactions including π - π interaction, hydrogen bonding, and metal-ligand coordination on controlling and tuning the molecular packing conformation of the corresponding self-assembled aggregates. Additional support for

this point comes from the IR spectroscopic, X-ray diffraction (XRD), transmission electronic microscopy (TEM), and scanning electron microscopy (SEM) results as detailed below.

IR spectra

The IR spectra of the two meso-tetrakis(4-hydroxyphenyl)porphyrin derivatives **1** and **2** together with their self-assembled nanostructures are shown in Fig. S1 and S2 (ESI[†]). For the purpose of comparative study, those for metal-free tetra(phenyl)porphyrin **3** were also recorded and are given in Fig. S3 (ESI[†]). The similar feature in the IR spectra of the nanostructures to that of the corresponding compounds for both H₂THPP (**1**) and CuTHPP (**2**) unambiguously confirms the composition of nanostructures from the corresponding porphyrin compounds. In the IR spectra of H₂THPP (**1**) and CuTHPP (**2**), two relatively broad absorptions at *ca.* 3280 and 3300 cm⁻¹, which are absent from that for **3**, are assigned to the hydrogen bonding stretching vibration.³³ This is also true for the IR spectra of the aggregates formed from both **1** and **2** in water, Fig. S1 and S2 (ESI[†]). Nevertheless, the absorption at 1229 cm⁻¹ in the IR spectra of both **1** and **2** is clearly due to the C–O vibration, Fig. S1 and S2 (ESI[†]).³⁴ A similar band is observed at 1229 cm⁻¹ in the IR spectrum of the aggregates formed from metal-free porphyrin **1** in water, Fig. S1 (ESI[†]). However, in the IR spectrum of the aggregates formed from porphyrinato copper complex **2** in water, this absorption band is broadened and shifts to lower frequency at 1219 cm⁻¹, indicating the formation of Cu–O metal–ligand coordination between the hydroxyl oxygen in the meso-attached phenyl groups in the porphyrin molecule with the copper center of a neighboring molecule in the nanostructure of **2**.³⁵ These results are in line with the X-ray diffraction (XRD) result as detailed below, suggesting the significant effect of hydrogen-bonding and metal–ligand coordination interactions on the formation of molecular aggregates of **1** and **2**.

Morphology of aggregates

The morphologies of aggregates formed were examined by transmission electronic microscopy (TEM) and scanning electron microscopy (SEM). Samples were prepared by casting a drop of sample solution onto a carbon-coated grid. In accordance with spectroscopic analysis results, different morphologies were observed for nanostructures fabricated from compounds **1–3**, Fig. 3.

As shown in Fig. 3E and F, depending mainly on the intermolecular π – π interaction in cooperation with the van der Waals interaction, molecules of metal-free tetra(phenyl)porphyrin **3** self-assemble in methanol into nanostructures with belt-like morphology with lengths of several micrometers and *ca.* 300 nm width. However, as shown in Fig. 3A, large nano-scale hollow spheres with an average diameter of *ca.* 70 nm were formed in water depending mainly on the intermolecular π – π interaction in cooperation with hydrogen bonding interaction of metal-free tetrakis(4-hydroxyphenyl)porphyrin **1**. The high magnification TEM image in the inset of Fig. 3A shows the thickness of these hollow spheres is in the range of 20–30 nm. Further evidence to confirm the hollow sphere nanostructures comes from the SEM image shown in Fig. 3B. As can be seen, the products are well-

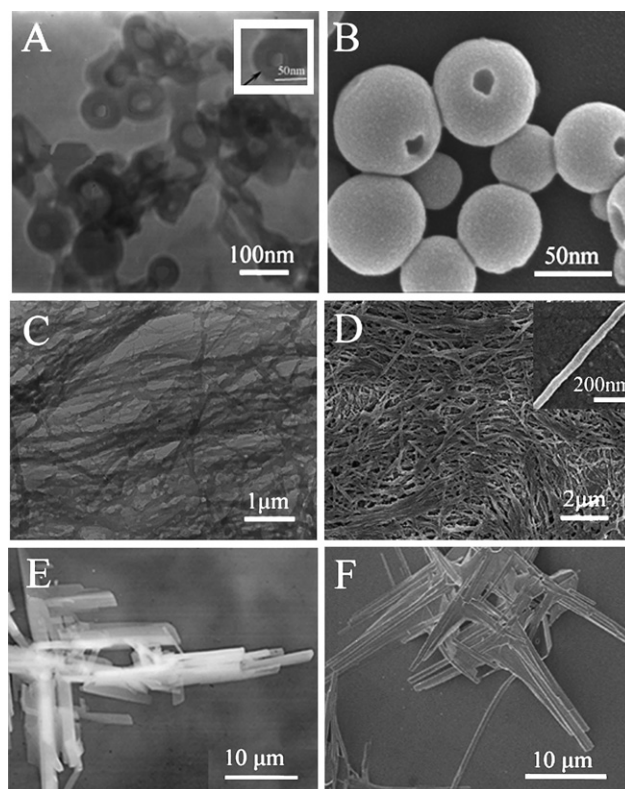


Fig. 3 TEM and SEM images of self-assembled nanostructures of compounds **1–3**. nano-scale hollow spheres formed from **1** in water observed by TEM (A) and SEM (B); nanoribbons formed from complex **2** observed by TEM (C) and SEM (D); nanobelts formed from **3** in methanol observed by TEM (E) and SEM (F).

defined hollow structures. There is typically just one hole in the surface of each nano-scale hollow sphere, which is favorable for their applications in drug delivery, chemical storage, light filters, chemical catalysis, and cosmetic foundations.³⁶ In contrast, as displayed in Fig. 3C and D, with the introduction of copper ion with a preferred coordination number of 6 into the hole of the porphyrin ring, the molecules of tetrakis(4-hydroxyphenyl)porphyrinato copper complex **2** self-assemble into nanostructures with ribbonlike morphology due to the formation of Cu–O metal–ligand coordination bonding between the hydroxyl groups at meso-attached phenyl substituents of one porphyrin molecule and the copper center of a neighboring porphyrin molecule in the self-assembly process of this complex. These one-dimensional nanoribbons as clearly shown in the inset of Fig. 3D display uniform size with *ca.* 70 nm width and 10 μ m length which may have potential applications in photovoltaics and field effect transistors.¹³ The distinct morphologies obtained for the self-assembly of these molecules reflect the differences of the porphyrin molecules in the *J* versus *H* aggregation mode and reveal the totally different molecular packing conformations as discussed below.

X-Ray diffraction patterns

The nanostructures of the two tetrakis(4-hydroxyphenyl)porphyrin derivatives **1** and **2** were fabricated by injecting a small volume of 1 mM methanol solution into a large volume of

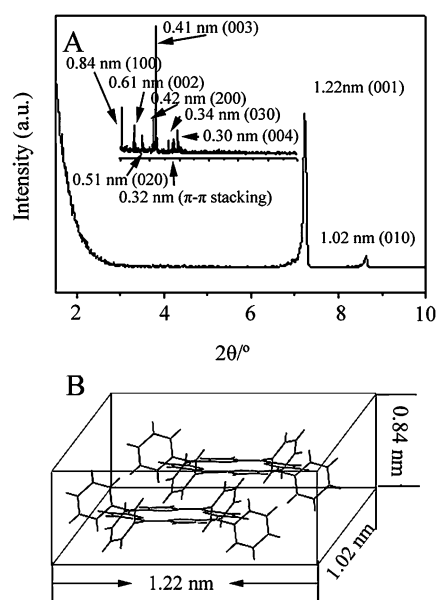


Fig. 4 (A) XRD profile and (B) schematic representation of the unit cell in the aggregates of compound 3.

water, while those of metal-free tetra(phenyl)porphyrin **3** were prepared by injecting its chloroform solution into methanol. The internal structures of self-assembled nanostructures of these porphyrin compounds were further investigated by X-ray diffraction (XRD) analysis, Fig. 4–6.

As shown in Fig. 4A, in the low angle range, the XRD diagram of the nanobelts formed from metal-free tetra(phenyl)porphyrin **3** shows a strong refraction peak at $2\theta = 7.23^\circ$ (corresponding to 1.22 nm) and a weaker refraction at 1.02 nm, which are ascribed to the refractions from the (001) and (010) planes, respectively. The (001) plane gives its higher order refractions at 0.61 (002), 0.41 (003) and 0.30 (004) nm, respectively, in the wide angle range of the XRD pattern. In addition, the wide angle range of the XRD pattern displays another sharp refraction at 0.84 nm, originating from the (100) plane, with its higher order refraction at 0.42 (200) nm. These diffraction results could be assigned to the refractions from a parallelepipedal lattice with the cell parameters of $a = 1.22$ nm, $b = 1.02$ nm, $c = 0.84$ nm, Fig. 4B. As can be seen from Fig. 4B, the dimensional size for a metal-free porphyrin H_2TPP molecule is 1.08 nm (length and width) \times 0.21 nm (height) according to the single crystal X-ray diffraction analysis result.³⁷ On the basis of the XRD result and the single crystal X-ray diffraction molecular structure, the unit cell consisting of two molecules is given for metal-free H_2TPP (**3**), Fig. 4B. It is worth noting that in the wide angle region, the nanobelt XRD pattern of H_2TPP (**3**) presents another sharp refraction at 0.32 nm, which is attributed to the stacking distance between tetrapyrrole cores of neighboring porphyrin molecules along the direction perpendicular to the tetrapyrrole rings.^{38–40} Actually, the stacking distance between neighboring porphyrin ligands in single crystals of H_2TPP (**3**) is 0.35 nm according to single crystal X-ray diffraction analysis.³⁷

As shown in Fig. 5A, in the low angle range, the XRD diagram of the nano-scale hollow spheres formed from tetrakis(4-hydroxyphenyl)porphyrin **1** shows a well-defined refraction peak

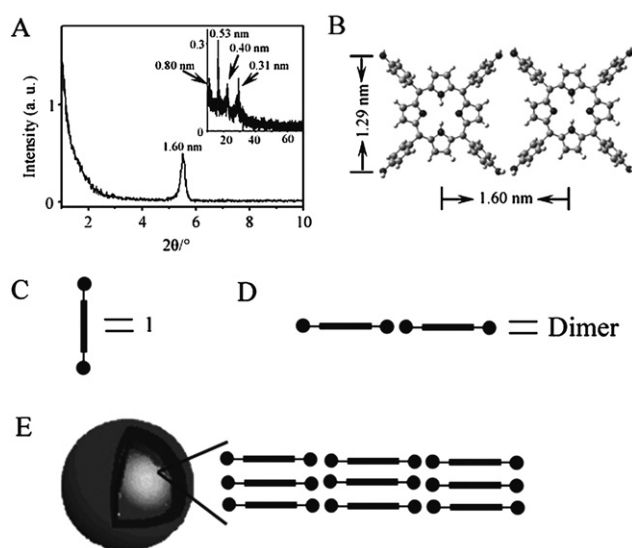


Fig. 5 (A) XRD profile of the aggregates of compound **1**; (B) molecular size of **1** optimized at the B3LYP/6-31G(d) level; (C) schematic representation of **1**; (D) schematic representation of a dimer **1**; and (E) schematic illustration of a hollow sphere formed in methanol with a close-up of the membrane showing the proposed structure.

at $2\theta = 5.52^\circ$ (corresponding to 1.60 nm), which is ascribed to the refraction from the (001) plane. This (001) plane gives its higher order refractions at 0.80 (002), 0.53 (003), and 0.40 (004) nm, respectively, in the wide angle region of the XRD pattern. On the basis of the geometry optimization and energy minimized molecular structure of H_2THPP (**1**) using the Gaussian 98 program at the B3LYP/6-31G(d) level,⁴¹ the length of the molecule is *ca.* 1.29 nm, Fig. 5B. Considering the average hydrogen bonding distance between neighboring porphyrin rings, 0.25–0.34 nm, obtained according to the single crystal X-ray diffraction analysis,⁴² the sharp peak observed at 1.60 nm in the XRD diagram of nano-scale hollow spheres formed from **1** in water can therefore be assigned to the length from the hydroxyl group of one porphyrin to the hydroxyl group of the neighboring one as shown in Fig. 5B. These results therefore indicate the formation of the ordered *J*-type aggregates, revealing the head-to-tail molecular arrangement in the membrane of the nano-scale hollow spheres of **1** due to the dominant hydrogen bonding interaction between the neighboring molecules. It is worth noting that the sharp diffraction peak observed at 0.31 nm for the nano-scale hollow spheres of **1** corresponds to the stacking distance between neighboring tetrapyrrole rings along the direction perpendicular to the porphyrin rings, in line with previous results.^{38–40} According to these experimental results, the formation mechanism of the nano-scale hollow spheres of **1** was proposed as displayed in Fig. 5C, D, and E. It is well known that in selective solvents, amphiphilic molecules like liposomes form micellar or vesicular supramolecular structures that would normally belong to the superstrong segregation limit mainly owing to the different solubilities of the hydrophilic and hydrophobic units.⁴³ As indicated by the IR spectroscopic result of the self-assembled nano-scale hollow spheres obtained from this metal-free porphyrin, during the molecular self-assembly process of H_2THPP (**1**)

a dimeric supramolecular structure is formed first through an intermolecular hydrogen bond between two hydroxyl groups of porphyrinato molecules. This formed dimer is amphiphilic in nature because of the hydrophilic hydroxyl groups and hydrophobic residual section, which then as the building block further self-assembles into the target hollow spheres depending mainly on the π - π interaction between tetrapyrrole rings.

In line with the electronic microscopic result, a comparatively different XRD diagram was obtained for compound **2**, Fig. 6A. From the diagram, it can be seen that in the low angle range, the XRD diagram of the nanoribbons shows two relatively broad refraction peaks at 1.52 and 1.06 nm, respectively, originating from the (001) and (010) planes. In addition, the wide angle range of XRD pattern displays another sharp refraction at 0.33 nm and one wide refraction at 0.25 nm, which are considered to be the π - π stacking distance between porphyrin molecules and the metal-ligand coordination bond length between the hydroxyl group of one molecule and the copper center of a neighboring porphyrinato copper molecule.^{31,44} According to the single crystal X-ray diffraction analysis,⁴⁵ Fig. 6B, the length of the molecule is about 1.54 nm, which is longer than that obtained from XRD. It therefore suggests that the planar structure of the porphyrin ligand gets distorted when the axial metal coordination formed between the hydroxyl group of meso-attached substituents of one porphyrin molecule and the copper metal center of a neighboring porphyrin molecule.⁴⁶ Furthermore, the diffraction peak at 1.06 nm corresponds to the distance from the C atom at the most peripheral position of the phenyl group to the same C atom position at the neighboring phenyl group. Taking the experimental results into account, the self-assembly mechanism was postulated for the formation of nanoribbons from **2** in water, Fig. 6C. Due to the competition and cooperation between hydrogen bonding and metal coordination interaction, a dimeric supramolecular structure, in which the Cu-O coordination bond between the hydroxyl oxygen in the meso-attached phenyl groups in the porphyrinato copper molecule with the copper

center of a neighboring molecule of **2**, was first formed. This is further unambiguously demonstrated by the X-ray photoelectron spectroscopic result as detailed below. Subsequently this bifunctional dimer analogue could polymerize through the same monomer-monomer interaction to pack in a one-dimensional direction. As a consequence, a ribbonlike morphology was obtained from this complex during the self-assembly process of **2**. This result is in good accordance with that for porphyrinato zinc complexes as revealed by single crystal X-ray diffraction analysis.^{23,47}

To further confirm the intermolecular coordination bond existed between the hydroxyl oxygen in the meso-attached phenyl groups in the porphyrinato copper molecule with the copper center of a neighboring molecule in the aggregates of porphyrinato copper complex **2**, X-ray photoelectron spectroscopy (XPS) was employed to identify the copper ion circumstance. The samples for recording XPS spectra were obtained by depositing a solution of compound **2** in methanol and the aggregates fabricated from **2** in methanol and water on the silicon surface and the spectra are shown in Fig. S4 (ESI[†]). As expected, both the monomeric compound **2** and its aggregates show typical signals for Cu²⁺ in their XPS spectra.⁴⁸ However, as clearly shown in Fig. S4 (ESI[†]), all the Cu²⁺ XPS intensity for the aggregates of **2** is significantly shifted in the lower bonding energy direction in comparison with those of the monomeric compound **2**, indicating the change of Cu²⁺ circumstance after the self-assembly process and confirming the rationality of the self-assembly mechanism discussed above.

Conclusion

In summary, the self-assembly properties of typical amphiphilic metal-free meso-tetrakis(4-hydroxyphenyl)porphyrin H₂THPP (**1**) and meso-tetrakis(4-hydroxyphenyl)porphyrinato copper complex CuTHPP (**2**) have been studied and compared with those of tetra(phenyl)porphyrin H₂TTP (**3**). Comparative investigation results reveal that besides the π - π interaction, competition and/or cooperation between the inter-molecular hydrogen bonding and metal-ligand coordination bonding lead to different molecular packing conformations and in turn different nanostructure morphologies in the self-assembly process. Intermolecular π - π interaction of metal-free porphyrin **3** leads to the formation of nanobelts. Hydrogen bonding together with π - π interaction dominates the formation of nano-scale hollow spheres for metal-free porphyrin compound **1**, while the additional dominant Cu-O coordination bond between the hydroxyl oxygen in meso-attached phenyl groups in the porphyrinato copper molecule with the copper center of a neighboring molecule of **2** leads to the formation of nanoribbons for this complex. The result presented here represents part of our continuous efforts towards understanding the relationship between synergistic interplay of noncovalent interactions including π - π interaction, metal-ligand coordination bonding, and hydrogen bonding in controlling and tuning the morphology of self-assembled nanostructures of porphyrin derivatives through molecular modification. They are believed to be helpful in opening new possibilities for the construction of molecular-based nanoelectronics and nanophotonics.

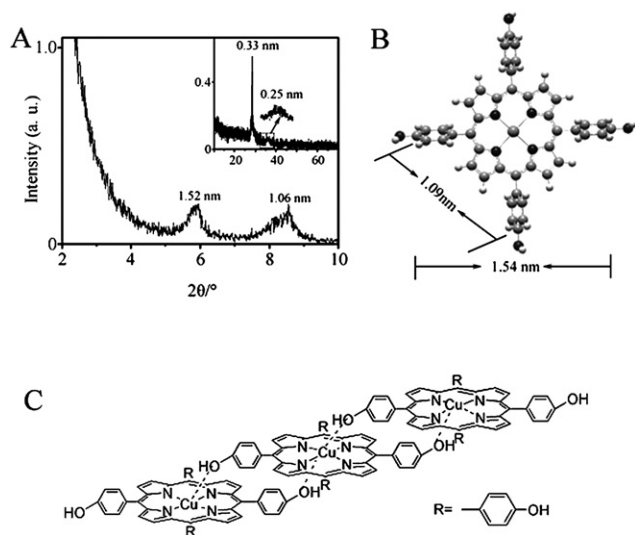


Fig. 6 (A) XRD profiles of the aggregates of compound **2**; (B) molecular size of **2** obtained from the single crystal X-ray diffraction analysis; and (C) schematic illustration of the aggregation mode of **2**.

Experimental

Measurements

MALDI-TOF mass spectra were carried out on a Bruker APEX47e ultra-high resolution. Elemental analyses were performed by the Institute of Chemistry, Chinese Academy of Sciences. Electronic absorption spectra were recorded on Hitachi U-4100 spectrophotometer. Fourier transform ion cyclotron resonance (FT-IR) mass spectrometer with α -cyano-4-hydroxycinnamic acid as matrix. Copper elemental analysis was performed by X-ray photoelectron spectroscopy (XPS) on PHI 5300 ESCA System (Perkin-Elmer, USA). The excitation source is Al K α radiation. Low-angle X-ray diffraction (XRD) measurements were carried out on a Rigaku D/max-cB X-ray diffractometer. TEM images were taken on a JEOL JEM-100CX II electron microscope operated at 100kV. SEM images were obtained using a JEOL JSM-6700F field-emission scanning electron microscopy. For SEM imaging, Au (1–2 nm) was sputtered onto the grids to prevent charging effects and to improve image clarity.

Materials

DMF was distilled from anhydrous MgSO₄ under reduced pressure prior to use. And the water used in the experiment is the ultrapure water. Column chromatography was carried out on silica gel (Merck, Kieselgel 60, 200–300 mesh) with the indicated eluent. All other reagents and solvents were of reagent grade and used as received. The compounds H₂TPP, H₂THPP, and CuTHPP were prepared according to literature methods.^{26,28}

Preparation of nanoaggregates

The nanoaggregates of the porphyrin derivatives **1–3** were fabricated by the phase transfer method according to the following procedure.^{4,8,22,23} A minimum volume (30–50 μ L) of concentrated methanol solution of compounds **1**, **2** (1 mM) (chloroform solution for **3**) was injected rapidly into 1 mL water (methanol for **3**). This clear solution was used to record the electronic absorption spectra for the aggregates. It is worth noting that the electronic absorption spectra of the complexes in water do not change significantly along with the increase of the quiescent time of the solution till 8 h at room temperature (25 °C). After being kept at room temperature for 24 h, suspensions were observed in the solution. These precipitates were transferred to the carbon-coated grid by pipetting for the TEM and SEM observations. These procedures and results were reproducible under the experimental conditions described above.

Acknowledgements

Financial support from the Natural Science Foundation of China, Ministry of Education of China, and Shandong University is gratefully acknowledged. We are also grateful to the Shandong Province High Performance Computing Centre for a grant of computer time.

References

- P. G. Schouten, J. M. Warman, M. P. de Haas, M. A. Fox and H. L. Pan, *Nature*, 1991, **353**, 736.
- J.-M. Lehn, *Science*, 2002, **295**, 2400.
- H. Gan, H. Liu, Y. Li, Q. Zhao, Y. Li, S. Wang, T. Jiu, N. Wang, X. He, D. Yu and D. Zhu, *J. Am. Soc. Chem.*, 2005, **127**, 12452.
- K. Balakrishnan, A. Datar, T. Naddo, J. Huang, R. Oitker, M. Yen, J. Zhao and L. Zang, *J. Am. Chem. Soc.*, 2006, **128**, 7390.
- D. M. Vriezema, J. Hoogboom, K. Velonia, K. Takazawa, P. C. M. Christianen, J. C. Maan, A. E. Rowan and R. J. M. Nolte, *Angew. Chem. Int. Ed.*, 2003, **42**, 772.
- For reviews see (a) D. Y. Yan, Y. F. Zhou and J. Hou, *Science*, 2004, **303**, 65; (b) J.-S. Hu, Y.-G. Guo, H.-P. Liang, L.-J. Wan and L. Jiang, *J. Am. Chem. Soc.*, 2005, **127**, 17090; (c) T. Shimizu, M. Masuda and H. Minamikawa, *Chem. Rev.*, 2005, **105**, 1401; (d) L. Zhi, T. Gorelik, Y. Wu, X. Kolb and K. Müllen, *J. Am. Chem. Soc.*, 2005, **127**, 12792; (e) Q. Liu, Y. Li, H. Liu, Y. Chen, X. Wang, Y. Zhang, X. Li and J. Jiang, *J. Phys. Chem. C*, 2007, **111**, 7298.
- R. Charvet, D. L. Jiang and T. Aida, *Chem. Commun.*, 2004, 2664.
- Y. Li, X. Li, Y. Li, H. Liu, S. Wang, H. Gan, J. Li, N. Wang, X. He and D. Zhu, *Angew. Chem. Int. Ed.*, 2006, **45**, 3639.
- For examples see (a) K. Zupan, L. Herenyi, K. Toth, Z. Majer and G. Csik, *Biochemistry*, 2004, **43**, 9151; (b) K. Zupan, L. Herenyi, K. Toth, M. Egyeki and G. Csik, *Biochemistry*, 2005, **44**, 15000.
- P. J. Stang and B. Olenyuk, *Acc. Chem. Res.*, 1997, **30**, 502.
- (a) T. Imamura and K. Fukushima, *Coord. Chem. Rev.*, 2000, **198**, 133; (b) J. Wojaczyński and L. Latos-Grażyński, *Coord. Chem. Rev.*, 2000, **204**, 113.
- K. S. Suslick, P. Bhyrappa, J.-H. Chou, M. E. Kosal, S. Nakagaki, D. W. Smithenry and S. R. Wilson, *Acc. Chem. Res.*, 2005, **38**, 283.
- J. Yu, S. Mathew, B. S. Flavel, M. R. Johnston and J. G. Shapter, *J. Am. Chem. Soc.*, 2008, **130**, 8788.
- R. Takahashi and Y. Kobuke, *J. Am. Chem. Soc.*, 2003, **125**, 2372.
- M. E. Kosal, J.-H. Chou, S. R. Wilson and K. S. Suslick, *Nat. Mater.*, 2002, **1**, 118.
- C. F. Van Nostrum and R. J. M. Nolte, *Chem. Commun.*, 1996, 2385.
- H. Engelkamp, S. Middelbeek and R. J. M. Nolte, *Science*, 1999, **284**, 785.
- J. A. A. W. Elemans, A. E. Rowan and R. J. M. Nolte, *J. Mater. Chem.*, 2003, **13**, 2661.
- P. Samori, H. Engelkamp, P. de Witte, A. E. Rowan, R. J. M. Nolte and J. P. Rabe, *Angew. Chem. Int. Ed.*, 2001, **40**, 2348.
- P. Samori, H. Engelkamp, P. A. J. de Witte, A. E. Rowan, R. J. M. Nolte and J. P. Rabe, *Adv. Mater.*, 2005, **17**, 1265.
- J. Sly, P. Kasák, E. Gomar-Nadal, C. Rovira, L. Górriz, P. Thordarson, D. B. Amabilino, A. E. Rowan and R. J. M. Nolte, *Chem. Commun.*, 2005, 1255.
- G. Lu, Y. Chen, Y. Zhang, M. Bao, Y. Bian, X. Li and J. Jiang, *J. Am. Chem. Soc.*, 2008, **130**, 11623.
- Y. Gao, X. Zhang, C. Ma, X. Li and J. Jiang, *J. Am. Chem. Soc.*, 2008, **130**, 17044.
- Y. N. Konan, R. Cerny, J. Favet, M. Berton, R. Gurny and E. Allémann, *Eur. J. Pharm. Biopharm.*, 2003, **55**, 115.
- Y. N. Konan, M. Berton, R. Gurny and E. Allémann, *Eur. J. Pharm. Science.*, 2003, **18**, 241.
- (a) A. D. Adler, F. R. Longo and W. Shergalis, *J. Am. Chem. Soc.*, 1964, **86**, 3145; (b) A. D. Adler, F. R. Longo, J. D. Finarelli, J. Goldmacher, J. Assour and L. Korsakoff, *J. Org. Chem.*, 1967, **32**, 476.
- (a) H. Guo, J. Jiang, Y. Shi, Y. Wang, J. Liu and S. Dong, *J. Phys. Chem. B*, 2004, **108**, 10185; (b) H. Guo, J. Jiang, Y. Shi, Y. Wang, Y. Wang and S. Dong, *J. Phys. Chem. B*, 2006, **110**, 587.
- A. D. Adler and F. R. Longo, *J. Inorg. Nucl. Chem.*, 1970, **32**, 2443.
- (a) X. Gong, T. Milic, C. Xu, J. D. Batteas and C. M. Drain, *J. Am. Chem. Soc.*, 2002, **124**, 14290; (b) N. C. Maiti, S. Mazumdar and N. Periasamy, *J. Phys. Chem. B*, 1998, **102**, 1528; (c) C. A. Hunter and J. K. M. Sanders, *J. Am. Chem. Soc.*, 1990, **112**, 5525; (d) K. Kano, H. Minamizono, T. Kitae and S. Negi, *J. Phys. Chem. A*, 1997, **101**, 6118; (e) R. Purrello, L. Monsu' Scolaro, E. Bellacchio, S. Gurrieri and A. Romeo, *Inorg. Chem.*, 1998, **37**, 3647.
- A. Ulman and J. Manassen, *J. Am. Chem. Soc.*, 1975, **97**, 6540.
- M. Kasha, H. R. Rawls and M. A. El-Bayoumi, *Pure Appl. Chem.*, 1965, **11**, 371.

- 32 K. Kano, K. Fukuda, H. Wakami, R. Nishiyabu and R. F. Pasternack, *J. Am. Chem. Soc.*, 2000, **122**, 7494.
- 33 (a) M. Kimura, T. Muto, H. Takimoto, K. Wada, K. Ohta, K. Hanabusa, H. Shirai and N. Kobayashi, *Langmuir*, 2000, **16**, 2078; (b) M. Kimura, T. Kuroda, K. Ohta, K. Hanabusa, H. Shirai and N. Kobayashi, *Langmuir*, 2003, **19**, 4825.
- 34 (a) J. Pan and K. L. Nguyen, *Anal. Chem.*, 2007, **79**, 2259; (b) M. B. Sayed, *Ind. Eng. Chem. Res.*, 2004, **43**, 4822.
- 35 T. S. Balaban, M. Linke-Schaetzl, A. D. Bhise, N. Vanthuynne, C. Roussel, C. E. Anson, G. Buth, A. Eichhofer, K. Foster, G. Garab, H. Gliemann, R. Goddard, T. Javorfi, A. K. Powell, H. Rosner and T. Schimmel, *Chem. Eur. J.*, 2005, **11**, 2267.
- 36 (a) F. Caruso, A. R. Caruso and H. Möhwald, *Science*, 1998, **282**, 1111; (b) F. Caruso, *Adv. Mater.*, 2001, **13**, 11; (c) Y. R. Ma, L. M. Qi, J. M. Ma and H. M. Cheng, *Langmuir*, 2003, **19**, 4040; (d) T. Nakashima and N. Kimizuka, *J. Am. Chem. Soc.*, 2003, **125**, 6386.
- 37 K. Kano, K. Fukuda, H. Wakami, R. Nishiyabu and R. F. Pasternack, *J. Am. Chem. Soc.*, 2000, **122**, 7494.
- 38 B. A. Minch, W. Xia, C. L. Donley, R. M. Hernandez, C. Carter, M. D. Carducci, A. Dawson, D. F. O'Brien and N. R. Armstrong, *Chem. Mater.*, 2005, **17**, 1618.
- 39 Z. Belarbi, C. Sirlin, J. Simon and J. J. Andre, *J. Phys. Chem.*, 1989, **93**, 8105.
- 40 M. Kimura, K. Wada, K. Ohta, K. Hanabusa, H. Shirai and N. Kobayashi, *J. Am. Chem. Soc.*, 2001, **123**, 2438.
- 41 M. J. Frisch, G. W. Trucks, H. B. Schlegel, G. E. Scuseria, M. A. Robb, J. R. Cheeseman, J. A. Montgomery, Jr., T. Vreven, K. N. Kudin, J. C. Burant, J. M. Millam, S. S. Iyengar, J. Tomasi, V. Barone, B. Mennucci, M. Cossi, G. Scalmani, N. Rega, G. A. Petersson, H. Nakatsuji, M. Hada, M. Ehara, K. Toyota, R. Fukuda, J. Hasegawa, M. Ishida, T. Nakajima, Y. Honda, O. Kitao, H. Nakai, M. Klene, X. Li, J. E. Knox, H. P. Hratchian, J. B. Cross, C. Adamo, J. Jaramillo, R. Gomperts, R. E. Stratmann, O. Yazyev, A. J. Austin, R. Cammi, C. Pomelli, J. W. Ochterski, P. Y. Ayala, K. Morokuma, G. A. Voth, P. Salvador, J. J. Dannenberg, V. G. Zakrzewski, S. Dapprich, A. D. Daniels, M. C. Strain, O. Farkas, D. K. Malick, A. D. Rabuck, K. Raghavachari, J. B. Foresman, J. V. Ortiz, Q. Cui, A. G. Baboul, S. Clifford, J. Cioslowski, B. B. Stefanov, G. Liu, A. Liashenko, P. Piskorz, I. Komaromi, R. L. Martin, D. J. Fox, T. Keith, M. A. Al-Laham, C. Y. Peng, A. Nanayakkara, M. Challacombe, P. M. W. Gill, B. Johnson, W. Chen, M. W. Wong, C. Gonzalez, and J. A. Pople, *Gaussian 03*, Revision B.05; Gaussian, Inc., Pittsburgh, PA, 2003.
- 42 (a) Y. Diskin-Posner, G. K. Patra and I. Goldberg, *CrystEngComm*, 2002, **4**, 296; (b) R. Krishna Kumar, S. Balasubramanian and I. Goldberg, *Inorg. Chem.*, 1998, **37**, 541; (c) M. Mazzanti, M. Veyrat, R. Ramasseul, J. C. Marchon, I. Turowska-Tyrk, M. Shang and W. R. Scheidt, *Inorg. Chem.*, 1996, **35**, 3733; (d) K. M. Barkigia, M. W. Renner, M. O. Senge and J. Fajer, *J. Phys. Chem. B.*, 2004, **108**, 2173.
- 43 M. Antonietti and S. Förster, *Adv. Mater.*, 2003, **15**, 1323.
- 44 Y.-F. Yang, Y.-S. Ma, L.-R. Guo and L.-M. Zheng, *Cryst. Growth Des.*, 2008, **8**, 1213.
- 45 I. Goldberg, H. Krupitsky, Z. Stein, Y. Hsiou and C. E. Strouse, *Supramolecular Chemistry*, 1994, **4**, 203.
- 46 T. S. Balaban, A. Eichhöfer and J.-M. Lehn, *Eur. J. Org. Chem.*, 2000, 4047.
- 47 D. Bonifazia, G. Accorsic, N. Armaroli, F. Songb, A. Palkarib, L. Echevoyen, M. Scholla, P. Seilera, B. Jauna and F. Diederich, *Helvetica Chimica. Acta.*, 2005, **88**, 1839.
- 48 V. Bolis, S. Maggiorini, L. Meda, F. D'Acapito, G. Turnes Palomino, S. Bordiga and C. Lamberti, *J. Chem. Phys.*, 2000, **113**, 9248.